Check for updates

View Article Online
View Journal

Dalton Transactions

Accepted Manuscript

This article can be cited before page numbers have been issued, to do this please use: M. G. Richmond, Kh. M. Uddin, Md. A. Chowdhury, Md. K. Hossain, S. Ghosh, D. A. Tocher and S. E. Kabir, *Dalton Trans.*, 2017, DOI: 10.1039/C7DT02933K.


This is an Accepted Manuscript, which has been through the Royal Society of Chemistry peer review process and has been accepted for publication.

Accepted Manuscripts are published online shortly after acceptance, before technical editing, formatting and proof reading. Using this free service, authors can make their results available to the community, in citable form, before we publish the edited article. We will replace this Accepted Manuscript with the edited and formatted Advance Article as soon as it is available.

You can find more information about Accepted Manuscripts in the author guidelines.

Please note that technical editing may introduce minor changes to the text and/or graphics, which may alter content. The journal's standard Terms & Conditions and the ethical guidelines, outlined in our author and reviewer resource centre, still apply. In no event shall the Royal Society of Chemistry be held responsible for any errors or omissions in this Accepted Manuscript or any consequences arising from the use of any information it contains.

ROYAL SOCIETY OF CHEMISTRY

rsc.li/dalton

Please do not adjust margins

View Article Online
DOI: 10.1039/C7DT02933K

Journal Name

ARTICLE

Published on 14 September 2017. Downloaded by University College London on 26/09/2017 10:08:13.

# Alkyne activation and polyhedral reorganization in benzothiazolate-capped osmium clusters on reaction with diethyl acetylenedicarboxylate (DEAD) and ethyl propiolate

Received 00th January 20xx,
Accepted 00th January 20xx

DOI: 10.1039/x0xx00000x

www.rsc.org/

Kh. Mahid Uddin,[a] Md. Arshad H. Chowdhury,[a] Md. Kamal Hossain,[a] Shishir Ghosh,[a] Derek A. Tocher,[b] Michael G. Richmond,[c,†] and Shariff E. Kabir[a]

The reactivity of the face-capped benzothiazolate clusters $HOs_3(CO)_9[\mu_3\text{-}C_7H_3(R)NS]$ (**1a,** R = H; **1b,** R = 2-$CH_3$) with alkynes has been investigated. **1a** reacts with DEAD at 67 °C to furnish the isomeric alkenyl clusters $Os_3(CO)_9(\mu\text{-}C_7H_4NS)(\mu_3\text{-}EtO_2CCCHCO_2Et)$ (**2a** and **3a**). X-ray crystallographic analyses of **2a** and **3a** have confirmed the stereoisomeric relationship of these products and the regiospecific polyhedral expansion that follows the formal transfer of the hydride to the coordinated alkyne ligand in $HOs_3(CO)_9(\mu\text{-}C_7H_4NS)(\eta^2\text{-DEAD})$. The significant structural differences between the two isomers, as revealed by the solid-state structures, derives from the regiospecific cleavage of one of the three Os-Os bonds in the intermediate alkenyl cluster $Os_3(CO)_9(\mu\text{-}C_7H_4NS)(\eta^1\text{-}EtO_2CCCHCO_2Et)$, which follows hydride transfer to the coordinated alkyne ligand in the pi compound $HOs_3(CO)_9(\mu\text{-}C_7H_4NS)(\eta^2\text{-DEAD})$. Control experiments confirm the reversibility of the reaction leading to the formation of **2a** and **3a**. Whereas heating either isomer in refluxing THF or benzene affords a binary mixture containing **2a** and **3a**, thermolysis in refluxing toluene leads to the activation of the alkenyl ligand and formation of the new cluster $Os_3(CO)_9(\mu\text{-}C_7H_4NS)(\mu_3\text{-}EtO_2CCCH_2)$ (**4**). **4** was independently synthesized from **1a** and ethyl propiolate at room temperature. The computed mechanisms that account for the formation of **2a** and **3a** are presented, along with the mechanism for the reaction of **1a** with ethyl propiolate to give **4**.

## Introduction

The reactivity of trimetallic clusters towards alkynes has been extensively studied over the past several years in an effort to better understand the available binding modes of unsaturated organic fragments at trimetallic centers.[1-30] The adopted binding mode and reactivity of the coordinated alkyne ligand are dependent on the nature of the triangular metal cluster and the substituents on the alkyne.[2,3] Thus, terminal alkynes, HC≡CR, react with the labile trinuclear metal cluster $Os_3(CO)_{10}(NCMe)_2$ to give the triply bridging alkyne compound $Os_3(CO)_{10}(\mu_3\text{-}\eta^2\text{-}HC{\equiv}CR)$. The initial pi complex is reactive, and the alkynyl CH group undergoes hydrogen transfer to the metal, giving $Os_3H(CO)_9(\mu_3\text{-}\eta^2\text{-alkyne})$ via a formal loss of CO and the oxidative addition of the alkyne C-H bond.[14,24] Use of internal alkynes, RC≡CR, furnishes alkyne-substituted clusters containing either a perpendicular $\mu_3\text{-}\eta^2$ (⊥) mode or, more commonly, a parallel $\mu_3\text{-}\eta^2$ (∥) mode of alkyne coordination. The perpendicular coordination mode is typically found in 46-electron clusters, while the parallel mode is observed in the vast majority of 48-electron clusters.[18,19,31,32] The reaction of the unsaturated hydrido-cluster $H_2Os_3(CO)_{10}$ with alkynes has also been the subject of numerous studies, and a wide variety of products are produced, the nature of which depends upon the particular alkyne employed.[14,23-30] Using acetylene, the μ-vinyl complex $HOs_3(CO)_{10}(\mu\text{-}\eta^2\text{-}CH{=}CH_2)$ is formed in high yield,[9,14] while use of the activated alkyne, $CF_3C{\equiv}CCF_3$, affords the zwitterionic complex $HOs_3(CO)_{10}(\mu_3\text{-}\eta^2\text{-}CF_3C{=}CHCF_3)$ in essentially quantitative yield and where the hydrocarbyl fragment caps one of the triangular faces of the cluster.[30]

The diverse outcomes observed in the reaction of $H_2Os_3(CO)_{10}$ with different alkynes are tangentially related to our earlier studies dealing with the reactivity of a series of electron-deficient triosmium clusters having the general formula $HOs_3(CO)_9(\mu_3\text{-}\eta^2\text{-L-H})$ (L = benzoheterocycle) with diazomethane. Despite the structural similarities of the starting clusters, the nature of the final product was extremely sensitive to the nature of the heterocyclic auxiliary.[33] For example, the reaction of the 2-methylbenzothiazolate-substituted cluster $HOs_3(CO)_9[\mu_3\text{-}\eta^2\text{-}C_7H_3(2\text{-}CH_3)NS]$ with $CH_2N_2$ yielded $Os_3(CO)_9[\mu\text{-}\eta^2\text{-}C_7H_3(2\text{-}CH_3)NS](\mu\text{-}CH_2)CH_3$, a rare example of a heterocyclic-substituted triosmium cluster containing an edge-

[a] Department of Chemistry, Jahangirnagar University, Savar, Dhaka-1342, Bangladesh.
[b] Department of Chemistry, University College London, 20 Gordon Street, London WC1H OAJ, UK.
[c] Department of Chemistry, University of North Texas, Denton, TX 76209, USA.
† Corresponding author: cobalt@unt.edu; 940-565-3515.

Electronic Supplementary Information (ESI) available: CCDC 1509600, 1509601, 1509603, and 1509602 contain the supplementary crystallographic data for compounds **2a**, **3a**, **3b**, and **4a**, respectively. These data can be obtained free of charge from The Cambridge Crystallographic Data Center via http://www.ccdc.cam.ac.uk/data_request/cif. Atomic coordinates of all DFT-optimized stationary points and spectroscopic data. See DOI:xxxxxxxxxxxxxx..

This journal is © The Royal Society of Chemistry 20xx



Please do not adjust margins

Dalton Transactions Accepted Manuscript

View Article Online
DOI: 10.1039/C7DT02933K


Published on 14 September 2017. Downloaded by University College London on 26/09/2017 10:08:13.

bridging methylene group and a σ-bound methyl group. In contrast, a similar reaction of the parent benzothiazolate-capped cluster $HOs_3(CO)_9(\mu_3\text{-}\eta^2\text{-}C_7H_4NS)$ afforded $H_2Os_3(CO)_9(\mu_3\text{-}\eta^2\text{-}CHC_7H_4NS)$, formed by insertion and the subsequent C-H oxidative addition of a $CH_2$ moiety into the heterocyclic ring C(7)-Os bond.[33b]

In keeping with our interest in fundamental bond formation reactions at metal clusters and the influence that heterocyclic auxiliaries have on metal clusters and their alkyne coordination, we have investigated the reaction of benzothiazolate-substituted cluster $HOs_3(CO)_9(\mu_3\text{-}C_7H_4NS)$ (**1a**) with the electron poor alkyne dimethyl acetylenedicarboxylate (DMAD).[34,35] Scheme 1 shows the initial alkyne addition products (**5** and **6**) that we isolated and structurally characterized from the reaction of **1a** and DMAD. **5** and **6** are isomers, and they demonstrate the coordinative flexibility of the alkyne to function as a multisite donor ligand that directly influences the selective opening of the cluster polyhedron.

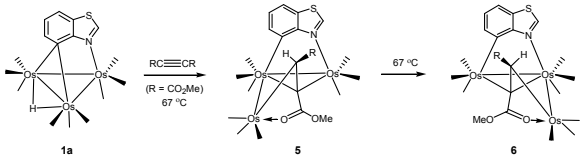


**Scheme 1.** Reaction of $HOs_3(CO)_9(\mu_3\text{-}C_7H_4NS)$ (1a) with dimethyl acetylenedicarboxylate (DMAD).

Control experiments established **5** as the product of kinetic control and subsequent heating verified its conversion to 6. Refluxing 6 in toluene led to further transformations involving the alkenyl moiety, with clusters **7** and **8** formed. Scheme 2 shows these clusters where the former product has undergone a *cis* to *trans* isomerization of the carbomethoxy groups, suggesting a reversible C-H bond activation involving the alkenyl moiety. The latter product results from a coupling of benzothiazolate and hydrocarbyl ligands. This functionalization of the heterocycle is accompanied by loss of two molecules of CO. The liberated CO derives from the cluster and decarboxylation of one of the carbomethoxy groups of the activated alkyne.

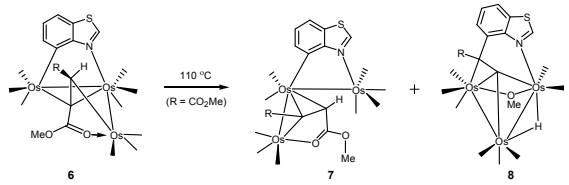


**Scheme 2.** Reactivity of **6** in refluxing toluene.

Wishing to explore the generality of the DMAD reaction with cluster **1a** with other activated alkynes, coupled with our interest in the possible functionalization of the metalated benzothiazolate ligand in **1a**, we have investigated the reaction of the electron poor alkynes diethyl acetylenedicarboxylate (DEAD) and ethyl propiolate with **1a** and the related benzothiazolate derivative $HOs_3(CO)_9[\mu_3\text{-}C_7H_3(2\text{-Me})NS]$ (**1b**). The observed reactivity differences are described, and the computed pathways leading to the new clusters **2a**, **3a**, and **4** are discussed.

## Results and discussion

### *Reactivity of 1a and 1b with DEAD*

The reaction of the benzothiazolate-capped cluster $HOs_3(CO)_9(\mu_3\text{-}C_7H_4NS)$ (**1a**) with excess diethyl acetylenedicarboxylate (DEAD) in refluxing THF furnishes the isomeric alkenyl complexes $Os_3(CO)_9(\mu\text{-}C_7H_4NS)(\mu_3\text{-}EtO_2CCCHCO_2Et)$ (**2a** and **3a**) as the major products in the reaction, as depicted in Scheme 3.

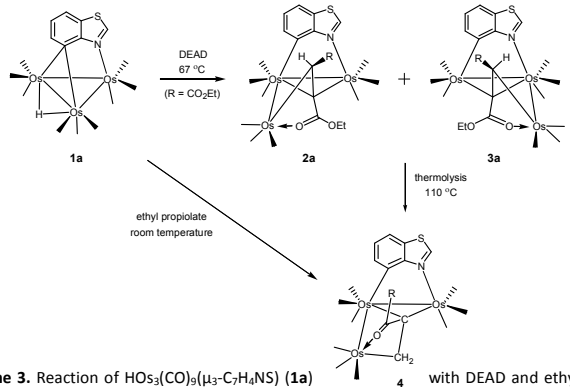


**Scheme 3.** Reaction of $HOs_3(CO)_9(\mu_3\text{-}C_7H_4NS)$ (**1a**) with DEAD and ethyl propiolate.

**2a** and **3a** are isomers, and they result from the selective opening of one of the osmium-osmium bonds in **1a**, following the formal transfer of the hydride to the coordinated alkyne ligand in the transient pi compound $HOs_3(CO)_9(\mu\text{-}C_7H_4NS)(\eta^2\text{-DEAD})$ (*vide infra*). The products were isolated by chromatography and characterized in solution by IR and $^1$H NMR spectroscopies, and the molecular structures of **2a** and **3a** were established by X-ray crystallography. **2a** exhibits six ν(CO) bands from 2088-1962 $cm^{-1}$ while **3a** reveals four ν(CO) bands from 2086-1986 $cm^{-1}$, confirming only the presence of terminal carbonyl stretching bands in both products. The $^1$H NMR spectrum recorded for **2a** shows two distinct methyl resonances at δ 1.16 and 1.29 and a 4H multiplet at δ 4.10 attributed to the methylene hydrogens of the carboethoxy groups. The 1H singlet at δ 2.51 is assigned to the alkenyl hydrogen. The four aryl hydrogens are readily assigned based on their couplings and chemical shift trends in related metalated clusters characterized by our groups. The lone hydrogen at C-2 on the benzothiazole ring appears as a singlet at δ 8.97, and the assignments for the ABC spin system for the remaining aryl hydrogens are illustrated Scheme 4. The ortho hydrogen adjacent to the metalated carbon is expected to appear downfield relative to the other hydrogens in this spin system[36] and may be confidently assigned as δ 7.79. The remaining two assignments follow from their first-order couplings and a $^1$H COSY experiment. The $^1$H NMR spectrum recorded for **3a**, whose selected chemical shift data are summarized in Scheme 4, is not unlike that of **2a**.

Dalton Transactions Accepted Manuscript


This journal is © The Royal Society of Chemistry 20xx

Please do not adjust margins
View Article Online
DOI: 10.1039/C7DT02933K


Published on 14 September 2017. Downloaded by University College London on 26/09/2017 10:08:13.

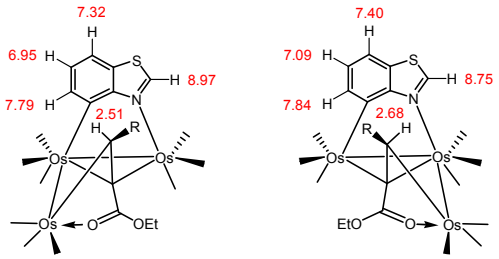


**Scheme 4.** $^1$H NMR assignments for the aryl and alkenyl hydrogens in **2a** and **3a**.

The isomeric nature of **2a** and **3a** was established by X-ray crystallography. The ORTEP diagram of the molecular structure of compound **2a** is shown in Fig. 1, whose caption includes selected bond distances and angles. The molecule contains an expanded triosmium core resulting from the formal cleavage of one of the three Os-Os bonds in **1a**. The coordination sphere in **2a** consists of nine terminal carbonyls, an edge-bridging benzothiazolate moiety ($C_7H_5NS$), and a triply bridging $EtO_2CCCHCO_2Et$ ligand. The carbonyls are equally distributed among three osmium atoms, and the metalated benzothiazolate ligand spans the Os(1)–Os(2) edge via the N(1) and C(16) atoms. The $EtO_2CCCHCO_2Et$ ligand, which effectively serves as a 5e donor, is covalently bonded to the Os(3) atom through the alkenyl carbon C(21), and the C(20) alkylidene atom serves to bridge the Os(1)-Os(2) vector. Coordination of the ester oxygen O(10) to the Os(3) center is also verified, and this completes the ligation of the three osmium atoms by the functionalization alkyne ligand. Overall, the molecule contains 50-valence electrons and exhibits two formal metal-metal bonds consistent with topological bonding rules of polyhedral clusters.[37] The Os(1)–Os(2) edge [2.8254(4) Å] that is simultaneously bridged by the heterocyclic and hydrocarbyl ligands is significantly shorter than the Os(2)–Os(3) vector [2.9318(4) Å]. The C(20)–C(21) bond distance of 1.529(8) Å is typical of an $sp^3$-$sp^3$ C-C single bond.[38] The functionalization and multisite coordination of the DEAD ligand contribute to the observed elongation of the alkyne C≡C functionality and its formal reduction to a C-C single bond. The molecular structure of **2a** is analogous to that of **5** (Scheme 1) obtained from the reaction of **1a** with DMAD in refluxing hexane. The Os–C, Os–N and Os–O bond distances found in **2a** are very similar to the corresponding bond distances observed in **5**.[34] Shown alongside **2a** in Fig. 1 is the DFT-optimized structure of **2a** (species **G**). The calculated structure for **G** exhibits good agreement with the solid-state structure.

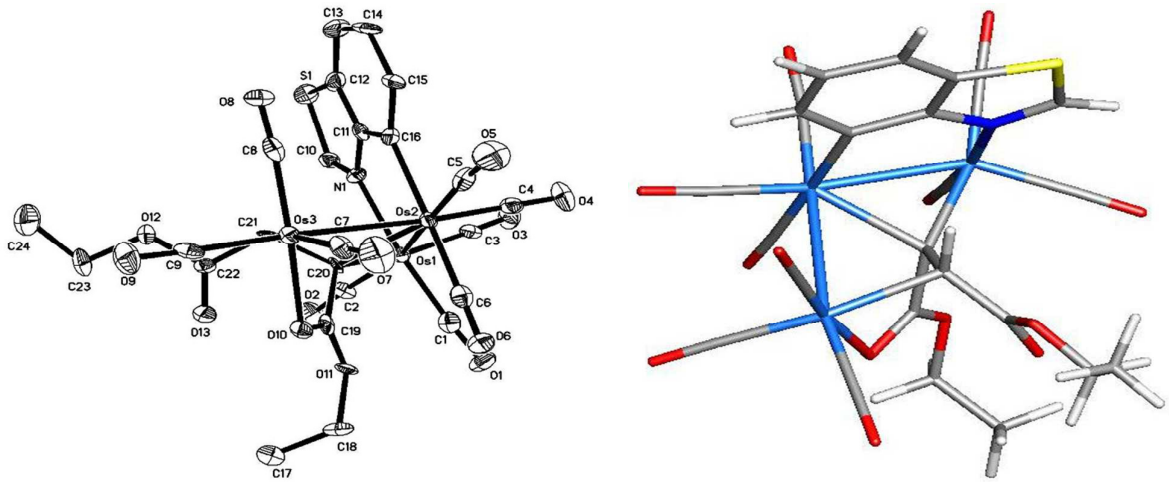


**Fig. 1.** ORTEP drawing of the molecular structure of **2a** (left) showing 50% probability thermal ellipsoids and DFT-optimized structure of **G** (right). Selected interatomic distances (Å) and angles (°) for **2a**: Os(1)–Os(2) 2.8254(4), Os(2)–Os(3) 2.9318(4), Os(3)–O(10) 2.161(5), Os(1)–N(1) 2.153(5), Os(2)–C(16) 2.158(7), Os(1)–C(20) 2.113(6), Os(2)–C(20) 2.265(6), Os(3)–C(21) 2.176(6), C(20)–C(21) 1.529(8), Os(1)–Os(2)–Os(3) 106.246(11), C(20)-Os(1)–Os(2) 52.20(16), C(20)-Os(2)–Os(1) 47.49(15), Os(1)–C(20)–Os(2) 80.31(19), C(21)-Os(3)–Os(2) 74.36(16).

The X-ray diffraction structure of **3a** is shown in Fig. 2. Two crystallographically independent molecules were found in the unit cell of **3a**. No significant structural differences exist, and we show only one of the molecules in the figure. The structure of **3a**, which is similar in nature to cluster **6** (Scheme 1), confirms its stereoisomeric nature vis-à-vis **2a**. Selected bond distances and angles are reported in the figure caption, and these data closely mirror those bond distance and angles reported for **2a** and the DMAD-based clusters **5** and **6**.[34] We have also optimized the structure of **3a** by DFT calculations, and species **M** is depicted in Fig. 2. While the coordination mode displayed by the $EtO_2CCCHCO_2Et$ ligand in **2a** and **3a** is similar, the regiospecific opening of one of the three Os-Os bond in cluster **1a** represents the principal architectural difference between the two products. The DFT calculations reveal a 0.2 kcal/mol preference for species **M** over **G**. The $\Delta G$ value for the DEAD-based products **2a** and **3a** is admittedly small and lies in the direction reported in our earlier DMAD reaction where the thermodynamic preference for cluster **6** versus **5** was demonstrated.

Dalton Transactions Accepted Manuscript


Please do not adjust margins

View Article Online
DOI: 10.1039/C7DT02933K

# Journal Name

## ARTICLE

Published on 14 September 2017. Downloaded by University College London on 26/09/2017 10:08:13.

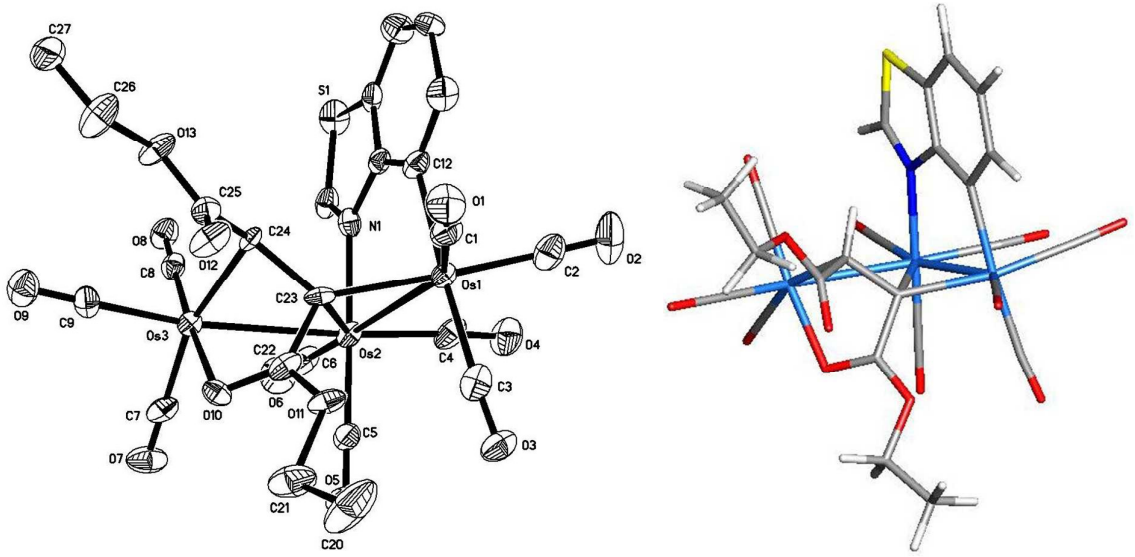


**Fig. 2.** The solid-state molecular structure of **3a** (left) showing 50% probability thermal ellipsoids and and DFT-optimized structure of **M** (right). Selected interatomic distances (Å) and angles (°) for **3a**: Os(1)–Os(2) 2.8434(6), Os(2)–Os(3) 2.9999(6), Os(3)–O(10) 2.151(5), Os(2)–N(1) 2.179(7), Os(1)–C(12) 2.136(8), Os(3)–C(24) 2.170(7), Os(1)–C(23) 2.107(7), Os(2)–C(23) 2.241(7), Os(1)–C(12) 2.136(8), C(23)–C(24) 1.540(10), C(24)–Os(3)–Os(2) 72.28(17), C(23)–Os(2)–Os(1) 47.14(19), C(23)–Os(1)–Os(2) 51.24(18), C(12)–Os(1)–Os(2) 86.7(2), N(1)–Os(2)–Os(1) 83.55(17), O(10)–Os(3)–Os(2) 85.13(13).

The effect of a methyl substituent on the heterocyclic auxiliary was next explored by using cluster **1b**. Treatment of **1b** with excess DEAD in refluxing THF furnished clusters **2b** and **3b** as the major products isolated upon chromatographic workup. Both **2b** and **3b** were fully characterized by spectroscopic methods, combustion analyses, and in the case of the latter product by X-ray diffraction analysis. Spectroscopically speaking, the recorded IR and $^{1}$H NMR spectra are consistent with the spectra recorded for **2a** and **3a**, and these data are summarized in the experimental section. The molecular structure of **3b**, which parallels that of **3a**, is shown in Fig. 3, with selected bond distances and angles quoted in the figure caption.

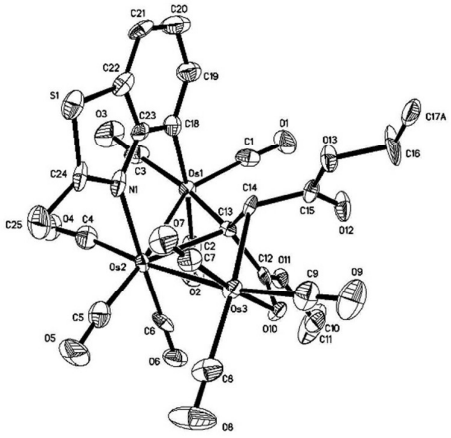


**Fig. 3.** The solid-state molecular structure of **3b** showing 50% probability thermal ellipsoids. Selected interatomic distances (Å) and angles (°): Os(1)–Os(2) 2.8429(3), Os(2)–Os(3) 2.9227(4), Os(3)–O(10) 2.144(4), Os(2)–N(1) 2.220(6), Os(1)–C(18) 2.136(7), Os(1)–C(13) 2.107(6), Os(2)–C(13) 2.267(6), Os(3)–C(14) 2.172(6), C(13)–C(14) 1.525(8), C(18)–Os(1)–Os(3) 86.74(19), Os(1)–C(13)–Os(2) 81.0(2), N(1)-Os(2)-Os(1) 83.28(15), C(14)–Os(3)–Os(2) 72.33(16), C(13)–Os(2)–Os(3) 60.14(14), C(13)–Os(1)–Os(2) 51.97(16), Os(1)–Os(2)–Os(3) 106.832(11).

Dalton Transactions Accepted Manuscript

Please do not adjust margins
View Article Online
DOI: 10.1039/C7DT02933K

Journal Name

ARTICLE

Published on 14 September 2017. Downloaded by University College London on 26/09/2017 10:08:13.

***Reversible interconversion between 2a and 3a and synthesis of 4 from thermolysis of 2a and 3a***

The equilibration of the products **2a** and **3a** was next investigated through a series of control experiments. Refluxing pure samples of either **2a** or **3a** in THF or benzene afforded binary mixtures of the isomers along with slow decomposition, as evidenced by the amount of material that remained at the origin of the TLC. The latter material appeared proportional to the reflux time The observation that each isomer readily equilibrates on heating confirms the reversible nature of their formation and the accessibility of a dynamic equilibrium between **2a** ⇌ **3a**. These results are consistent with our earlier study with DMAD where the equilibrium between **5** and **6** was established. We also examined the thermolysis of **2a** and **3a** at a higher temperature. Heating either isomer in refluxing toluene gave the new triosmium cluster $Os_3(CO)_9(\mu\text{-}C_7H_4NS)(\mu_3\text{-}EtO_2CCCH_2)$ (**4**) in low yield (< 12%) after chromatographic separation and recrystallization. TLC analysis of the final reaction solution confirmed the presence of several other products whose amounts were too small for characterization, in addition to considerable decomposition material that remained at the origin of the TLC plate. The mechanism for the formation of **4** from **2a** and **3a** remains unknown at this time and may proceed with the release of $CO_2$ and ethylene from one of the carboethoxy groups present in the starting isomeric clusters. Interestingly, the DMAD-substituted clusters **5** and **6** do not yield an analogue of **4** but rather clusters **7** and **8** under identical conditions. The different products observed in these reactions underscore the importance of the nature of the ester moiety in helping to direct the nature of the final thermolysis product. The coordinated alkenyl ligand in **4** may also be envisioned as arising from the reaction of the terminal alkyne ethyl propiolate and cluster **1a**. Accordingly, we performed this control experiment and report that the cluster **4** is produced slowly at room temperature upon treatment with ethyl propiolate. The reaction between **1a** and ethyl propiolate follows a Markovniko path for hydride insertion. The two different reaction paths that furnish **4** are depicted in Scheme 5.

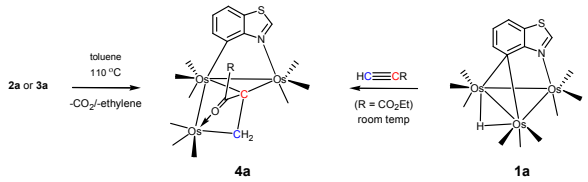


**Scheme 5.** Different reaction pathways that give cluster **4**.

**4** was characterized by a combination of IR and $^1$H NMR spectroscopies, and the solid-state structure was determined by single-crystal X-ray diffraction analysis. Cluster **4** contains 50-valence electrons, and the $CH_2$ moiety of the $EtO_2CCCH_2$ ligand derives from the formal hydrogen transfer from an ethyl moiety of one of the original $CO_2Et$ groups in the precursor isomer **2a**,**3a**. The ORTEP diagram of the molecular structure of **4** is shown in Fig. 4; the opened triangular core displayed by the three osmium atoms is in agreement with the 50e count present in **4**. The two Os-Os bonds exhibit distances of 2.8168(3) Å [Os(2)-Os3)] and 2.9271(4) Å [Os(1)-Os(2)] and display a mean distance of 2.8720 Å consistent with their single-bond designation. The benzothiazolate ligand bridges the Os(2)-Os(3) vector while the hydrocarbyl ligand $EtO_2CCCH_2$, which effectively serves as a 5e donor, ligates the three metal centers through the C(14), C(15), and O(10) atoms. The Os–C, Os–N and Os–O bond distances in compound **4** are similar to the corresponding bond distances in **2a**, **3a**,**b**, and the previously reported compounds **5** and **6**.[34] The geometry-optimized structure of **4** (species **S**) was also investigated by DFT, with the computed structure shown in Fig. 4, where excellent agreement with the experimentally determined structure was found.

Dalton Transactions Accepted Manuscript



Please do not adjust margins

View Article Online
DOI: 10.1039/C7DT02933K

Journal Name

ARTICLE

Published on 14 September 2017. Downloaded by University College London on 26/09/2017 10:08:13.

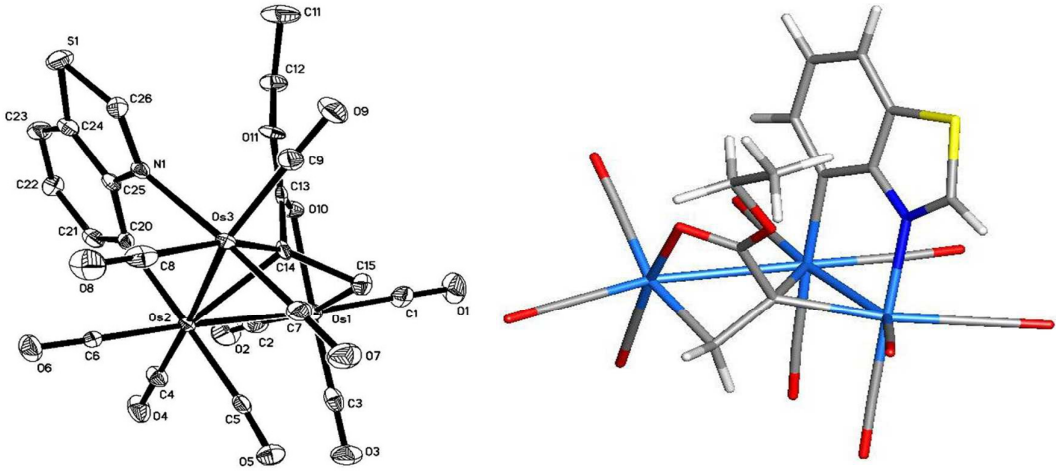


**Fig. 4.** ORTEP drawing of the molecular structure of **4** (left) showing 50% probability thermal ellipsoids and DFT-optimized structure of **S** (right). Selected interatomic distances (Å) and angles (°) for **4**: Os(1)–Os(2) 2.9271(4), Os(2)–Os(3) 2.8168(3), Os(1)–O(10) 2.167(4), Os(2)–C(14) 2.244(5), Os(3)–C(14) 2.114(5), Os(1)-C(15) 2.171(6), Os(2)-C(20) 2.144(5), Os(3)–N(1) 2.152(5), O(10)–Os(1)–Os(2) 86.09(10), C(15)–Os(1)–Os(2) 73.33(16), C(20)–Os(2)–Os(3) 87.32(15), C(14)–Os(2)–Os(3) 47.74(14), Os(3)–Os(2)–Os(1) 106.101(9), N(1)–Os(3)–Os(2) 83.31(12).

The IR spectrum of **4** exhibits six terminal ν(CO) bands from 2082-1955 $cm^{-1}$ and the $^1H$ assignments are summarized in Scheme 6. The diastereotopic methylene hydrogens associated with the alkenyl linkage appear as two distinct doublets at δ 3.09 and 3.00, each of which exhibits a geminal coupling of 7.4 Hz, while the methylene hydrogens in the ethyl group appear as two multiplets centered at δ 3.28 and 2.13. The spectral properties recorded for **4** are consistent with the solid-state structure.

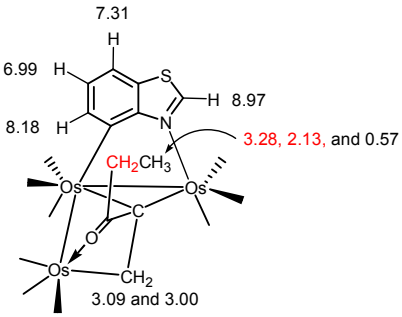


**Scheme 6.** $^1H$ NMR assignments for the hydrogens in **4**.

***Computed reaction mechanisms for the formation of 2a, 3a, and 4 from 1a and alkyne***

Earlier calculations from our group have addressed ligand addition to related $Os_3$ clusters possessing a bridging benzylidene moiety,[36,39] and these reports have demonstrated that the incoming ligand will add to one of the two originally metalated osmium centers. However, the possibility of a kinetically active cluster that contains an edge-bridging aryl moiety cannot be eliminated from consideration. A structural alteration through a reduction in hapicity of the benzothiazolate ligand from $\mu_3$ to $\mu$-$\eta^1$ coordination would give such an intermediate. This process is depicted in Scheme 7 using **1a** for illustrative purposes. The $\mu_3 \rightarrow \mu$-$\eta^1$ transformation creates a vacant coordination site at the exposed osmium atom, which in turn may react with the incoming ligand. Examples involving the addition of a 2e donor to cluster systems containing both face-capped and edge-bridged clusters have been computationally investigated by us and others.[40] The possibility of an opened form of **1a** as an entry point for the coordination of alkyne was duly explored.

Dalton Transactions Accepted Manuscript

Please do not adjust margins
View Article Online
DOI: 10.1039/C7DT02933K

Journal Name

ARTICLE

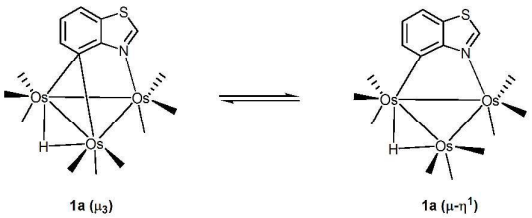


**Scheme 7.** Benzothiazolate ligand isomerization in **1a**.

The energetics for the $\mu_3 \rightarrow \mu\text{-}\eta^1$ opening of the benzothiazolate ligand in **1a** were examined by DFT, and here we initially optimized the structure of **1a** (**A**), which is shown in Fig. 5. A subsequent step-scan calculation on **A** was next performed, and one of the Os-C bonds in the metalated benzothiazolate ligand was incrementally increased, allowing us to obtain **TSAA_alt** and **A_alt**. As the Os-C bond is gradually lengthened during the calculation, the hydride residing below the $Os_3$ plane moves upward and adopts a coplanar orientation with the metallic frame. Coupled with the hydride movement is the tripodal rotation of the three CO ligands at the developing unsaturated $Os(CO)_3$ moiety. The optimized structure of this transition state is **TSAA_alt**, and it lies 18.9 kcal/mol above **A**. The resulting product is the opened cluster represented by **A_alt**, and it is 15.6 kcal/mol less stable than its isomeric counterpart containing a face-capping benzothiazolate ligand. The reaction of **A_alt** with DEAD (**B**) and ethyl propiolate (**N**) was next investigated by allowing each alkyne to approach the exposed $Os(CO)_3$ site in **A_alt**. In all step-scan calculations, the approaching alkyne promoted the collapse of the edge-bridging benzothiazolate ligand and regeneration of species **A**. Fortunately, a viable transition-state structure was computed for the direct addition of the alkynes **B** and **N** to **A**, as described below.

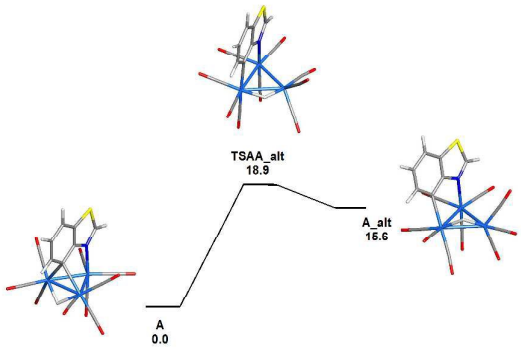


**Fig. 5.** Free-energy profile for the opening of the benzothiazolate moiety in **1a** (**A**) to give the unsaturated cluster $HOs_3(CO)_9(\mu\text{-}\eta^1\text{-}C_7H_4NS)$ (**A_alt**) through **TSAA_alt**. Energy values are in kcal/mol relative to **A**.

The addition of DEAD (**B**) to **A** was computationally investigated by DFT to elucidate the reaction paths leading to the observed reaction products **G** and **M**. Two distinct reaction paths were computed, and we discuss the formation of **G** first. Figures 6 and 7 show the DFT-optimized structures and the potential energy surface, respectively, en route to **G**. The reaction consists of five steps with the initial coordination of the alkyne **B** by **A** taking place via **TSABC**. Here the incoming alkyne approaches the starting cluster syn to one of the two metalated Os-C bonds. This trajectory promotes a $\mu_3 \rightarrow \mu\text{-}\eta^1$ transformation of the benzothiazolate ligand that facilitates the axial coordination of **B** on the same face of the metallic frame that is occupied by the heterocyclic ligand. **B** contains 48e and is coordinatively saturated. The resulting pi complex, represented by **C**, is 22.0 kcal/mol less stable than **A** and **B**. Next, **C** undergoes a rate-limiting reductive elimination (**TSCD**) and affords the alkenyl-substituted cluster **D**. Noteworthy features in **D** include the $\eta^1$ $CH(CO_2Et)C(CO_2Et)$ moiety, a bridging CO, and reformation of the $\mu_3$ benzothiazolate ligand. Dihedral rotation within the ester moiety bound to the metalated carbon in **D** gives **E** via **TSDE**. Once formed, species **E** experiences a polyhedral expansion through pi coordination of the $\eta^1$ alkenyl ligand. The net result of this transformation is the conversion of the alkenyl moiety from a 1e to a 3e donor. Coordination of the pendant ester oxygen that lies opposite the metallic plane containing the benzothiazolate ligand in **F** occurs via **TSFG**, followed by the observed product **G**. The overall reaction is exergonic and liberates 25.4 kcal/mol.

Published on 14 September 2017. Downloaded by University College London on 26/09/2017 10:08:13.
Dalton Transactions Accepted Manuscript

This journal is © The Royal Society of Chemistry 20xx


Please do not adjust margins

View Article Online
DOI: 10.1039/C7DT02933K

Journal Name

ARTICLE

Published on 14 September 2017. Downloaded by University College London on 26/09/2017 10:08:13.

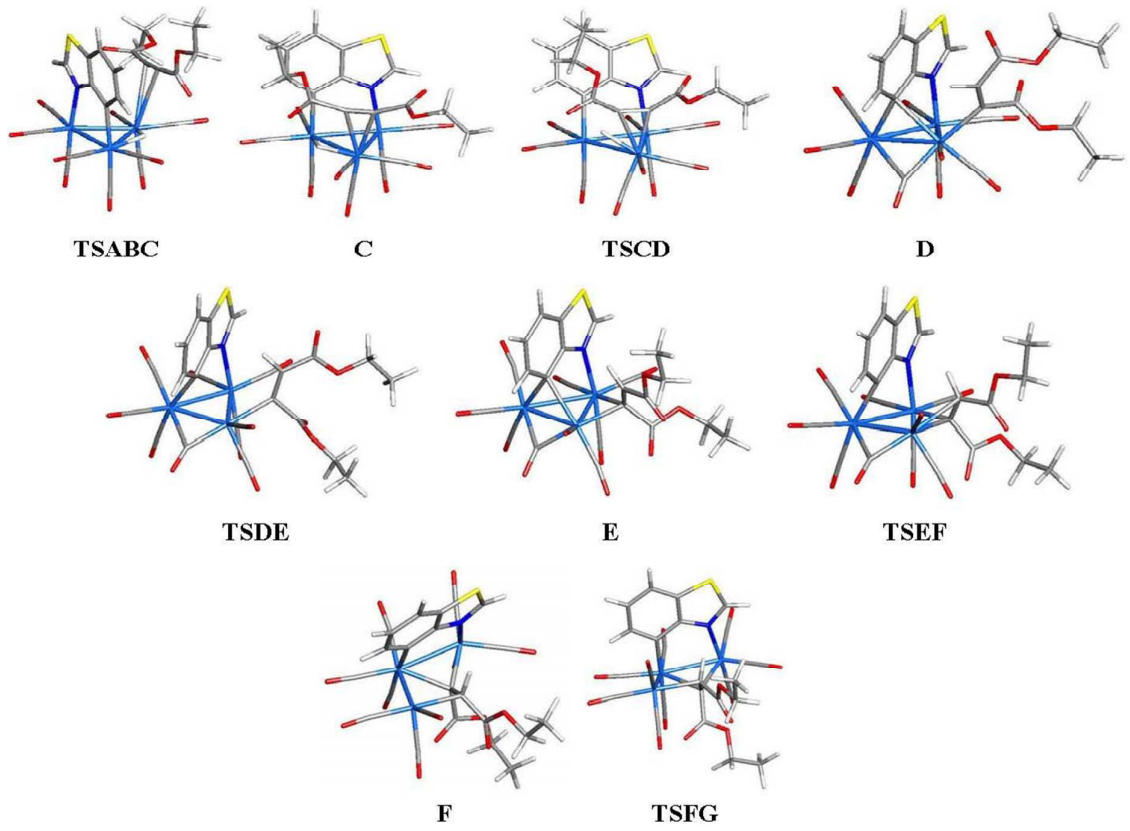


**Fig. 6.** DFT-optimized structures for **C**-**F** and the transition states **TSABC**, **TSCD**, **TSDE**, **TSEF**, and **TSFG**. The optimized structure for the alkyne DEAD (species **B**) is not shown.

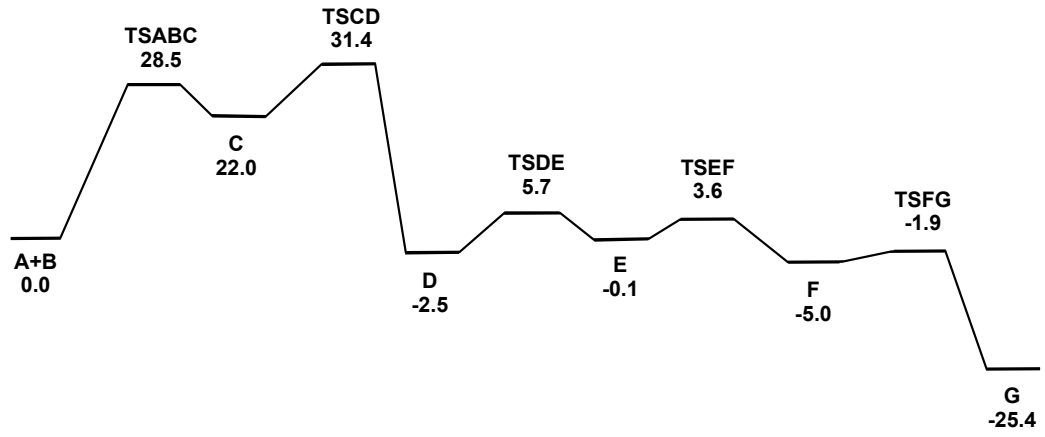


**Fig. 7.** Free energy surface for the conversion of **A** and **B** to **G**. Energy values are ΔG in kcal/mol with respect to **A** and **B**.

Dalton Transactions Accepted Manuscript

Please do not adjust margins
View Article Online
DOI: 10.1039/C7DT02933K

Journal Name

ARTICLE

Published on 14 September 2017. Downloaded by University College London on 26/09/2017 10:08:13.

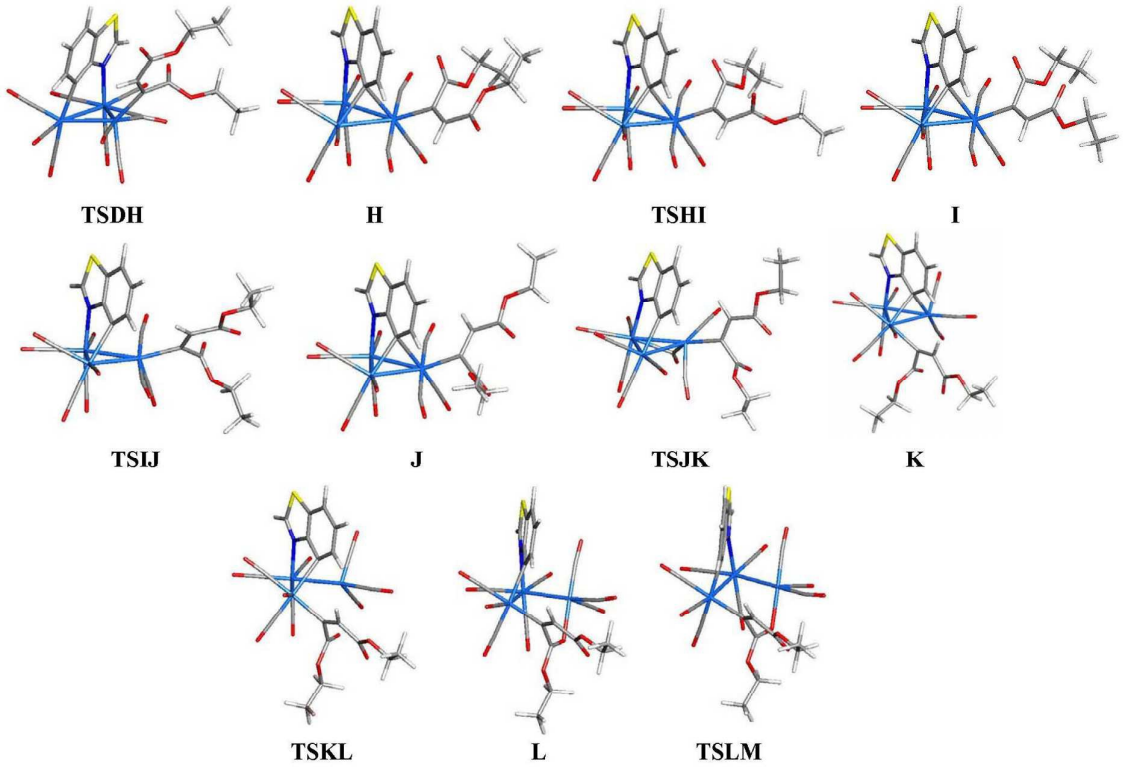


**Fig. 8.** DFT-optimized structures for **H**-**L** and the transition states **TSDH**, **TSHI**, **TSDE**, **TSIJ**, **TSJK**, **TSKL**, and **TSLM**.

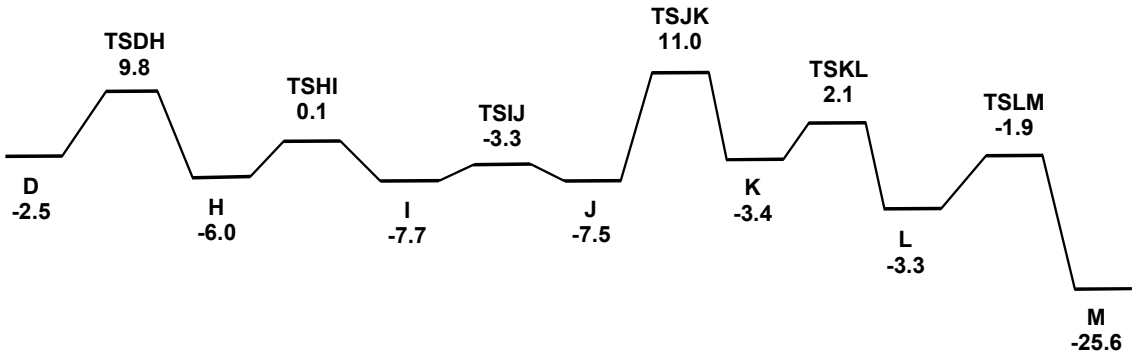


**Fig. 9.** Free energy surface for the conversion of **D** to **M**. Energy values are ΔG in kcal/mol with respect to **A** and **B**.

Dalton Transactions Accepted Manuscript



Please do not adjust margins

View Article Online
DOI: 10.1039/C7DT02933K



Published on 14 September 2017. Downloaded by University College London on 26/09/2017 10:08:13.

The formation of **M** traces its origin to **D** (*vide supra*). Figs. 8 and 9 show the optimized structures and the potential energy profile for the structures that give **M**. The evolution of **D** to **M** requires six steps, with the first three (**D** → **J**) consisting of torsional rotations within the $\eta^1$ alkenyl group (CH and ester moieties) which position this ligand for its subsequent migration across the Os-Os vector bridged by the metalated heterocycle. The transfer of the alkenyl group in **J** to the adjacent osmium atom in **K** occurs through the transition state **TSJK**. Of the six steps that follow the rate-limiting step **TSCD**, **TSJK** is the highest on this portion of the relatively flat potential energy surface (PES). This transformation is assisted by the concerted terminal-to-bridge migration of the axial CO at the $Os(CO)_3[\eta^1\text{-}CH(CO_2Et)C(CO_2Et)]$ moiety to the nitrogen-substituted osmium center, whose formation is discernable in **TSJK**. The ester oxygen atom in **K** next adds to adjacent the osmium center (the original site of the alkenyl ligand) bound by the edge-bridging benzothiazolate ligand. The coordination of the ester oxygen in **TSKL** occurs at the expense of an Os-Os bond and promotes the polyhedral expansion observed in **L**. The final step involves the coordination of the free pi bond in the $CH(CO_2Et)C(CO_2Et)$ ligand to the N- and O-bound osmium centers in **L** to give **M**. The formation of **M** from **A** and **B** is exergonic and releases 25.6 kcal/mol.

The empirically validated equilibration of **2a** and **3a** may now be rationalized within the framework of the computed energy surfaces that afford **G** and **M**. Heating either **2a** or **3a** will furnish a mixture of isomers since the net energy barrier back to **D** from either **G** or **M** is relatively low, and this ensures the facile formation of a binary mixture of products having the formula $Os_3(CO)_9(\mu\text{-}C_7H_4NS)(\mu_3\text{-}EtO_2CCCHCO_2Et)$. For the conversion of **G** to **D**, the energy barrier is 31.1 kcal/mol based on the difference in energy between **G** → **TSDE**, the latter which is the highest point on the PES en route to the pivotal intermediate **D**. The energy barrier for the conversion of **M** to **D** is 36.6 kcal/mol based on $\Delta G$ between **M** → **TSJK**. The barrier associated with the latter isomerization is 5.5 kcal/mol higher in energy compared to the reaction starting from **G**, and the computed energy difference parallels the qualitative observation that **2a** isomerizes more rapidly than **3a** when refluxed in THF. Refluxing both clusters in toluene, while promoting their isomerization, also leads to the decomposition of the clusters **2a** and **3a** along with the formation of cluster **4**.

The direct reaction of **1a** (**A**) with added ethyl propiolate (**N**) to give **4** (**S**) was examined by DFT. The addition of **N** to **A** is analogous to the reaction using DEAD (**B**) as a ligand. The optimized structures and intrinsic reaction coordinate for the ethyl propiolate reaction are shown in Figs. 10 and 11, respectively. The rate-limiting step is **TSOP**, and it involves the formation of the alkenyl bond in the reductive elimination step. The barrier height of this step is 33.6 kcal/mol and the resulting $\eta^1$ product **P** is 1.3 kcal/mol more stable than the starting materials. The **P** → **Q** interconversion involves a torsional rotation about the Os-C(alkenyl) vector that orients the alkenyl $CH_2$ moiety syn to the coordination nitrogen atom. This step places the $CH_2$ moiety in a suitable environment for its final destination below the metallic plane that is ligated by the edge-bridging benzothiazolate ligand in **S**, following the migration of the alkenyl ligand to the nitrogen-substituted osmium center in **R**. The conversion of **R** → **S** occurs via **TSRS** and here the 1e alkenyl moiety is transformed into a 5e donor ligand through coordination of both the alkenyl pi and ester oxygen groups. Concomitant with the coordination of these two donors is the $\mu_3 \rightarrow \mu\text{-}\eta^1$ opening of the benzothiazolate ligand to give **S**, whose formation is favorable and lies 19.4 kcal/mol below **A** and **N**.

Dalton Transactions Accepted Manuscript

Please do not adjust margins

View Article Online
DOI: 10.1039/C7DT02933K

Journal Name

ARTICLE

Published on 14 September 2017. Downloaded by University College London on 26/09/2017 10:08:13.

Dalton Transactions Accepted Manuscript

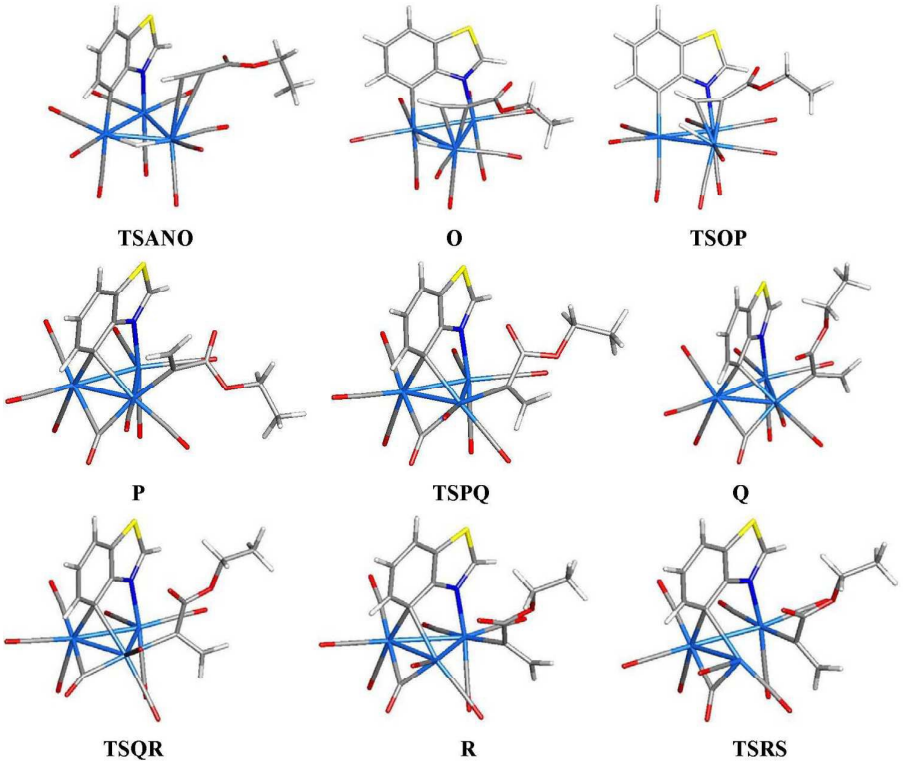


**Fig. 10.** DFT-optimized structures for **O**-**R** and the transition states **TSANO**, **TSOP**, **TSPQ**, **TSQR**, and **TSRS**. The optimized structure for ethyl propiolate (species **N**) is not shown.

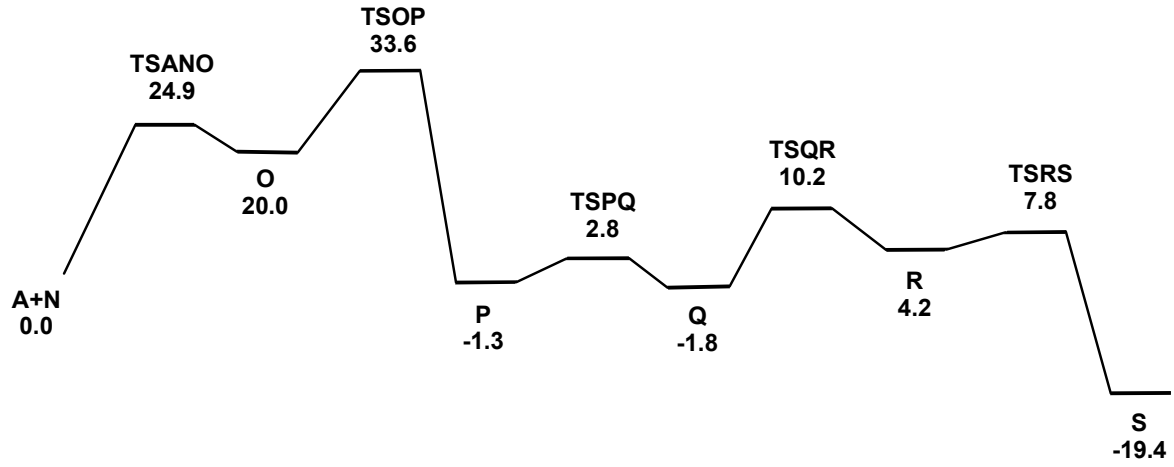


**Fig. 11.** Free energy surface for the conversion of **A** and **N** to **S**. Energy values are ΔG in kcal/mol with respect to **A** and **N**.

This journal is © The Royal Society of Chemistry 20xx



Please do not adjust margins

View Article Online
DOI: 10.1039/C7DT02933K



Journal Name

ARTICLE

Published on 14 September 2017. Downloaded by University College London on 26/09/2017 10:08:13.

## Conclusions

The reactions described in this study are summarized in Scheme 3. Coordination of the activated alkynes DEAD and ethyl propiolate by the benzothiazolate-capped clusters $HOs_3(CO)_9[\mu_3\text{-}C_7H_3(R)NS]$ (**1a,** R = H; **1b,** R = 2-$CH_3$) gives a pair of isomers **2a**,**b** and **3a**,**b** that differ primarily by selective polyhedral expansion of one of three metal-metal bonds. The isomeric clusters **2a** and **3a** may be equilibrated in refluxing THF or benzene, and this supports the coordinatively flexible nature of the triply bridged $EtO_2CCCHCO_2Et$ ligand. Through the use of DFT calculations, we have identified pertinent reaction intermediates and show that functionalization of the coordinated alkyne via reductive elimination with the ancillary hydride represents the rate-limiting step for the formation of **2a**, **3a**, and **4** starting from **1a** and alkyne. Future studies will center on the transfer of the alkenyl ligand to the heterocyclic auxiliary and the electronic influence the heterocycle has, if any, on controlling the reversible polyhedral expansion observed in our reactions.

## Experimental

#### General and instrumentation

All the reactions were carried out under a nitrogen atmosphere using standard Schlenk techniques unless otherwise stated. Reagent grade solvents were dried by the standard methods and freshly distilled prior to use. Diethyl acetylenedicarboxylate and ethyl propiolate were purchased from Acros Organics Chemicals Inc. and were used as received. Product separations were performed by TLC in the air on 0.5 mm silica gel 60 Å $F_{254}$ glass plates. Infrared spectra were recorded on a Shimadzu IR Prestige-21 spectrophotometer and $^1$H NMR spectra were recorded on a Bruker DPX 400 spectrometer. All NMR chemical shifts are reported in δ units and are referenced to the residual protons of the deuterated solvents. Elemental analyses were performed by the Microanalytical Laboratory of Wazed Miah Research Centre at Jahangirnagar University.

#### Reaction of $HOs_3(CO)_9(\mu_3\text{-}C_7H_4NS)$ (1a) with DEAD

To a THF solution (25 mL) containing **1a** (0.10 g, 0.11 mmol) was added diethyl acetylenedicarboxylate (90 mg, 0.53 mmol) under nitrogen flush. The reaction mixture was heated at 67 °C for 12 h during which time the solution color changed from green to yellow. The solvent was removed under reduced pressure and the residue subjected to TLC on silica gel. Elution with hexane/$CH_2Cl_2$ (1:1, v/v) developed three bands. The first band was unreacted **1a** (trace) while the second and third bands afforded $Os_3(CO)_9(\mu\text{-}C_7H_4NS)(\mu_3\text{-}EtO_2CCCHCO_2Et)$ (**2a**) (35 mg, 25%) and $Os_3(CO)_9(\mu\text{-}C_7H_4NS)(\mu_3\text{-}EtO_2CCHCO_2Et)$ (**3a**) (25 mg, 21%) as yellow crystals after recrystallization from hexane/$CH_2Cl_2$ at 4 °C. Data for **2a**: Anal. Calcd for $C_{24}H_{15}NO_{13}Os_3S$: C, 25.55; H, 1.34; N, 1.24. Found: C, 25.69; H, 1.43; N, 1.39. IR (*ν*CO, $CH_2Cl_2$): 2088 w, 2067 s, 2028 s, 1994 s, 1983 m, 1962 w cm$^{-1}$. $^1$H NMR ($CD_2Cl_2$): δ 8.97 (s, 1H), 7.79 (d, J 6.4, 1H), 7.32 (d, J 6.4, 1H), 6.95 (t, J 6.4, 1H), 4.10 (m, 4H), 2.51 (s, 1H), 1.29 (t, J 6.8, 3H), 1.16 (t, J 6.8, 3H). Data for **3a**: Anal. Calcd for $C_{24}H_{15}NO_{13}Os_3S$: C, 25.55; H, 1.34; N, 1.24. Found: C, 25.72; H, 1.52; N, 1.45. IR (*ν*(CO), $CH_2Cl_2$): 2086 m, 2065 s, 2031 s, 1989 s cm$^{-1}$. $^1$H NMR ($CD_2Cl_2$): δ 8.75 (s, 1H), 7.84 (d, J 7.6 Hz, 1H), 7.40 (d, J 7.6 Hz, 1H), 7.09 (t, J 7.6 Hz, 1H), 4.08 (m, 4H), 2.68 (s, 1H), 1.29 (t, J 7.2, 3H), 1.13 (t, J 7.2, 3H).

#### Thermal equilibation of 2a and 3a

**2a** (15 mg, 0.013 mmol) in 15 mL of THF was heated to reflux for 8 h, after which time the solution was allowed to cool. The solvent with concentrated under vaccum and the residue purified by chromatography, as described as above, to gave **3a** (7.5 mg, 50%) and unreacted **2a** (3.0 mg, 20%). Refluxing **3a** under analgous conditions gave **2a** and **3a** in isolated yields of (1.8 mg, 12%) and (7.9 mg, 53%), respectively.

#### Thermolysis of 3a

A toluene solution (20 mL) of **3a** (20 mg, 0.018 mmol) was heated to reflux for 5 h. The solvent was removed under reduced pressure upon cooling, and the residue subjected to TLC on silica gel. Elution with hexane/$CH_2Cl_2$ (1:1, v/v) developed four bands. The second band yielded $Os_3(CO)_9(\mu\text{-}C_7H_4NS)(\mu_3\text{-}EtO_2CCCH_2)$ (**4**) (3 mg, 12%) as yellow crystals after recrystallization from hexane/$CH_2Cl_2$ at 4 °C. The contents of the other three bands were too small for complete characterization. Data for **4**: Anal. Calcd for $C_{21}H_{11}NO_{11}Os_3S$: C, 23.88; H, 1.05; N, 1.33. Found: C, 24.12; H, 1.11; N, 1.40%. IR (*ν*(CO), $CH_2Cl_2$): 2082 m, 2060 vs, 2027 s, 1995 s 1973 s, 1955 w cm$^{-1}$. $^1$H NMR ($CD_2Cl_2$): *δ* 8.97 (s, 1H), 8.18 (d, J 7.2 Hz, 1H), 7.31 (d, J 7.2 Hz, 1H), 6.99 (t, J 7.2 Hz, 1H), 6.09 (d, J 7.2 Hz, 1H), 3.28 (m, 1H), 3.0 (d, J 7.4, 1H), 2.13 (m, 1H), 0.57 (t, J 7.2 Hz, 3H).

#### Reaction of 1a with ethyl propiolate

To **1a** (0.10 g, 0.11 mmol) in 25 mL of $CH_2Cl_2$ was added ethyl propiolate (90 mg, 0.53 mmol). The reaction was stirred at room temperature for 4 h during which time the color changed from green to yellow. After removal of the volatiles under reduced pressure the residue was purified by TLC. Elution with hexane/$CH_2Cl_2$ (1:1, v/v) developed five bands. The first band was unreacted **1a** (trace) and the third band afforded $Os_3(CO)_9(\mu\text{-}C_7H_4NS)(\mu_3\text{-}EtO_2CCCCH_2)$ (**4**) (24 mg, 21%). The contents of the other three bands were too small for complete characterization.

Dalton Transactions Accepted Manuscript

Please do not adjust margins
View Article Online
DOI: 10.1039/C7DT02933K


Published on 14 September 2017. Downloaded by University College London on 26/09/2017 10:08:13.

**Table 1** Crystallographic data and structure refinement details for compounds **2a**, **3a**, **3b** and **4**

| | **2a** | **3a** | **3b** | **4** |
|---|---|---|---|---|
| CCDC entry no | 1509600 | 1509601 | 1509603 | 1509602 |
| Cryst system | triclinic | triclinic | triclinic | triclinic |
| Space group | *P*-1 | *P*-1 | *P*-1 | *P*-1 |
| a, Å | 10.2449(3) | 10.047(2) | 9.841(3) | 10.2041(8) |
| b, Å | 11.0705(4) | 16.538(3) | 9.9715(3) | 10.8173(8) |
| c, Å | 13.4872(4) | 17.657(3) | 17.3201(5) | 11.4433(9) |
| α, deg | 78.130(3) | 75.769(2) | 75.059(3) | 76.534(1) |
| β, deg | 74.717(3) | 84.515(2) | 80.399(2) | 80.930(1) |
| γ, deg | 81.572(3) | 84.498(2) | 63.273(3) | 81.651(1) |
| V, Å$^3$ | 1437.09(8) | 2823.1(8) | 1464.30(8) | 1205.3(2) |
| Mol formula | $C_{24}H_{15}NO_{13}Os_3S$ | $C_{24}H_{15}NO_{13}Os_3S$ | $C_{25}H_{17}NO_{13}Os_3S$ | $C_{21}H_{11}NO_{13}Os_3S$ |
| fw | 1128.03 | 1128.03 | 1142.06 | 1055.97 |
| Formula units per cell (Z) | 2 | 4 | 2 | 2 |
| $D_{calcd}$ (Mg/m$^3$) | 2.607 | 2.654 | 2.590 | 2.910 |
| λ (Mo Kα), Å | 0.71073 | 0.71073 | 0.71073 | 0.71073 |
| μ (mm$^{-1}$) | 13.369 | 13.610 | 13.122 | 15.923 |
| F(000) | 1028 | 2056 | 1044 | 952 |
| Total reflections | 21344 | 24202 | 23960 | 9301 |
| Independent reflections | 5630 | 10939 | 5737 | 4660 |
| Data/res/parameters | 5603/0/382 | 10939/0/758 | 5737/0/391 | 4660/0/334 |
| GOF on $F^2$ | 1.049 | 1.040 | 1.054 | 1.113 |
| R1[a] [I ≥ 2σ(I)] | 0.0348 | 0.0403 | 0.0354 | 0.0260 |
| *w*R2[b] (all data) | 0.0862 | 0.1067 | 0.0808 | 0.0593 |
| Δρ(max), Δρ(min) (e/Å$^3$) | 3.04, -2.62 | 2.79, -1.89 | 2.18, -2.41 | 1.47, -1.56 |

[a]$R1 = \Sigma||F_o| - |F_c||/\Sigma|F_o|$; [b]$wR2 = \{\Sigma[w(F_o^2 - F_c^2)^2]/\Sigma[w(F_o^2)^2]\}^{1/2}$

Dalton Transactions Accepted Manuscript



Please do not adjust margins

View Article Online
DOI: 10.1039/C7DT02933K

Journal Name

ARTICLE

Published on 14 September 2017. Downloaded by University College London on 26/09/2017 10:08:13.

**Reaction of $HOs_3(CO)_9[\mu_3\text{-}C_7H_3(2\text{-}CH_3)NS]$ (1b) with DEAD**

To a THF solution (25 mL) containing **1b** (0.10 g, 0.11 mmol) was added diethyl acetylenedicarboxylate (90 mg, 0.53 mmol), after which time the reaction was heated at 67 °C for 24 h. After removal of the volatiles under reduced pressure the residue was subjected to TLC on silica gel. Elution with hexane/$CH_2Cl_2$ (1:1, v/v) developed three bands. The first band contained unreacted **1b** (trace), while the second and third bands afforded $Os_3(CO)_9[\mu\text{-}C_7H_4NS(CH_3)](\mu_3\text{-}EtO_2CCCHCO_2Et)$ (**3b**) (35 mg, 40%) and $Os_3(CO)_9[\mu\text{-}C_7H_4NS(CH_3)](\mu_3\text{-}EtO_2CCCHCO_2Et)$ (**2b**) (35 mg, 40%), respectively, as yellow crystals after recrystallization from hexane/$CH_2Cl_2$ at 4 °C. Data for **2b**: Anal. Calcd for $C_{25}H_{17}NO_{13}Os_3S$: C, 26.29; H, 1.50; N, 1.23. Found: C, 26.74; H, 1.63; N, 1.51%. IR ($\nu$(CO), $CH_2Cl_2$): 2088 w, 2067 s, 2028 s, 1994 s, 1983 m, 1962 w $cm^{-1}$. $^1H$ NMR (CDCl3): δ 7.76 (d, 1H, J 7.5 Hz), 7.01 (t, 1H, J 7.5 Hz, 1H), 7.27 (d, 1H, J 7.5 Hz), 4.18 (m, 4H), 2.86 (s, 3H), 1.30 (t, 3H, J 5.0 Hz), 0.88 (t, J 5.0 Hz, 3H). Data for **3b**: Anal. Calcd for $C_{25}H_{17}NO_{13}Os_3S$: C, 26.29; H, 1.50; N, 1.23. Found: C, 26.44; H, 1.63; N, 1.51%. IR ($\nu$(CO), $CH_2Cl_2$): 2085 w, 2063 vs, 2029 s, 1987 s $cm^{-1}$. $^1H$ NMR ($CDCl_3$): $\delta$ 7.77 (d, 1H, J 7.5 Hz), 7.30 (d, 1H, J 7.5 Hz), 7.03 (t, 1H, J 7.5 Hz), 4.18 (m, 4H), 2.89 (s, 3H), 1.33 (t, J 5.0 Hz, 3H), 1.19 (t, J 5.0 Hz, 3H).

**X-ray crystallography**

Crystals of **3a** and **4a** were mounted on a glass fiber and diffraction data collected on a Bruker SMART APEX diffractometer at 293 K (**3a**) and 150 K (**4a**) using Mo-Kα radiation (λ=0.71073 Å). Data collection, indexing, and cell refinements were done with SMART software, and data reduction and absorption correction used SAINT and SADAB,[41] respectively. Crystals of **2a** and **3b** were mounted on a nylon loop and diffraction data collected on an Agilent SuperNova Dual diffractometer at 150 K using Mo-Kα radiation (λ=0.71073 Å). Data collection, indexing, data reduction and absorption corrections were applied using CrysalisPro V171.[42] Structure solutions and refinements were carried out with SHELXS and SHELXL,[43] respectively. Non-hydrogen atoms were refined anisotropically and hydrogen atoms included with a riding model. Compound **3b** contains a disordered OEt group that was modeled over two sites. The details of the data collection and structure refinement are given in Table 1.

**Computational methodology and modeling details**

All DFT calculations were performed with the Gaussian 09 package of programs[44] using the B3LYP hybrid functional. This functional is comprised of Becke's three-parameter hybrid exchange functional (B3)[45] and the correlation functional of Lee, Yang, and Parr (LYP).[46] Each osmium atom was described with the Stuttgart-Dresden effective core potential and SDD basis set,[47] and the 6-31G(d') basis set[48] was employed for all remaining atoms.

All reported geometries were fully optimized, and analytical second derivatives were evaluated at each stationary point to determine whether the geometry was an energy minimum (no negative eigenvalues) or a transition structure (one negative eigenvalue). Unscaled vibrational frequencies were used to make zero-point and thermal corrections to the electronic energies, and the resulting free energies are reported in kcal/mol relative to the specified standard. Intrinsic reaction coordinate (IRC) calculations were performed on all transition-state structures in order to establish the reactant and product species associated with each transition-state structure. The geometry-optimized structures have been drawn with the *JIMP*2 molecular visualization and manipulation program.[49]

## Acknowledgments

SEK thanks the Ministry of Education, the Government of the Peoples' Republic of Bangladesh, and the University Grants Commission of Bangladesh for sponorship and financial support of this work. MGR thanks The Robert A. Welch Foundation through Grant B-1093 for research support. We also wish to acknowledge the computational resources at UNT that are housed in the High-Performance Computing Services (HPCS) and CASCaM facilities; NSF support (CHE-1531468) of the latter center is acknowledged. We also thank Prof. Michael B. Hall (TAMU) for providing us a copy of his *JIMP2* program.

## Notes and references

1 R.D. Adams, J.P. Selegue in *Comprehensive Organometallic Chemistry, Vol. 4* (Ed.: G. Wilkinson), Pergamon Press, Oxford, 1982, p. 1033.
2 D. Osella, P.R. Raithby in *Stereochemistry of Organometallic and Inorganic Compounds, Vol. 3* (Ed.: I. Bernal), Elsevier, Amsterdam, 1988.
3 E. Sappa, A. Tiripicchio, P. Braunstein, *Chem. Rev.* 1983, *83*, 203.
4 S.E. Kabir, G. Hogarth, *Coord. Chem. Rev.* 2009, *253*, 1285.
5 T. Takemori, A. Inagaki, H. Suzuki, *J. Am. Chem. Soc.* 2001, *123*, 1762.
6 A.D. Clucas, J.R. Shapley, S.R. Wilson, *J. Am. Chem. Soc.* 1981, *103* 7387.
7 J.F. Blount, L.F. Dahl, C. Hoogzand, W. Hiibel, *J. Am. Chem. Soc.* 1966, *88*, 292.
8 V. Busetti, G. Granozzi, S. Aime, R. Gobetto, D. Osella, *Organometallics* 1985, *3*, 1510.

Dalton Transactions Accepted Manuscript

Please do not adjust margins
View Article Online
DOI: 10.1039/C7DT02933K


Published on 14 September 2017. Downloaded by University College London on 26/09/2017 10:08:13.


9 M. Tachikawa, J.R. Shapley, C.G. Pierpont, *J. Am. Chem. Soc.* 1975, *97*, 7172.

10 S. Rivomanera, G. Lavigne, N. Lugan, J.-J. Bonnet, *Organometallics* 1991, *10*, 2285.

11 S. Aime, R. Gobetto, L. Milone, D. Osella, L. Violano, A.J. Arce, Y.D. Sanctis, *Organometallics* 1991, *10*, 2854.

12 A.J. Arce, Y.D. Sanctis, A.J. Deeming, *Polyhedron* 1988, *7*, 979.

13 M.I. Bruce, P.A. Humphrey, H. Miyamae, A.H. White, J. *Organomet. Chem.* 1991, *417*, 431.

14 A.J. Deeming, S. Hasso, M. Underhill, *J. Chem. Soc., Dalton Trans.* 1975, 1614.

15 A.J.P. Domingos, B.F.G. Johnson, J. Lewis, *J. Organomet. Chem.* 1972, *36*, C43.

16 D. Boccardo, M. Botta, R. Gobetto, D. Osella, A. Tiripicchio, M.T. Camellini, *J. Chem. Soc., Dalton Trans.* 1988, 1249.

17 S. Rivomanana, G. Lavigne, N. Lugan, J.-J. Bonnet, *Inorg. Chem.* 1991, *30*, 4110.

18 M.P. Brown, P.A. Dolby, M.M. Harding, A.J. Mathews, A.K. Smith, D. Osella, M. Arbrun, R. Gobetto, P.R. Raithby, P. Zanello, *J. Chem. Soc, Dalton Trans.* 1993, 827.

19 J.A. Clucas, P.A. Dolby, M.M. Harding, A.K. Smith, *J. Chem. Soc, Chem. Commun.* 1987, 1829.

20 M.R. Burke, J. Takats, *J. Organomet. Chem.* 1986, *302*, C25.

21 A.J. Deeming, A.M. Senior, *J. Organomet. Chem.* 1992, *439*, 177.

22 D. Osella, L. Pospisil, J. Fiedler, *Organometallics* 1993, *12*, 3140.

23 W.G. Jackson, B.F.G. Johnson, J.W. Kelland, J. Lewis, K.T. Schorp, *J. Organomet. Chem.* 1975, *88*, C17.

24 A.J. Deeming, *Adv. Organomet. Chem.* 1986, *26*, 1.

25 E. Rosenberg, E. Anslyn, L. Milone, S. Aime, R. Gobetto, D. Osella, *Gazz. Chim. Ital.* 1988, *118*, 299.

26 R.D. Adams, G. Chen, J.T. Tanner, *Organometallics* 1990, *9*, 1530.

27 E. Sappa, A. Tirripicchio, A.M. Manotti Lanfredi, *J. Organomet. Chem.* 1983, *249*, 391.

28 J.R. Shapley, *Inorg. Chem.* 1982, *21*, 3295.

29 R. Gobetto, L. Milone, F. Reineri, L. Salassa, A. Viale, E. Rosenberg, *Organometallics* 2002, *21*, 1919.

30 Z. Dawoodi, M.J. Mays, J. *Chem. Soc., Dalton Trans.* 1984, 1931

31 a) D. Osella, R. Gobetto, P. Montenegro, P. Zanello, A. Cinquantini, *Organometallics* 1985, *5*, 1247; b) B.E.R. Schilling, R. Hoffmann, *J. Am. Chem. Soc.* 1979, *101*, 3456; c) G. Granozzi, E. Tondello, M. Casarin, S. Aime, D. Osella, *Organometallics* 1983, *2*, 430; d) S. Aime, R. Bertoncello, V. Busetti, R. Gobetto, G. Granozzi, D. Osella, *Inorg. Chem.* 1986, *25*, 4004; e) C. Moreno, M.-L. Marcos, M.-J. Macazaga, J. Gomez-Gonzalez, R. Gracia, F. Benito-Lopez, E. Martínez-Gimeno, A. Arnanz, *Organometallics* 2011, *30*, 1838.

32 C. Moreno, M.-L. Marcos, M.-J. Macazaga, J. Gomez-Gonzalez, R. Gracia, F. Benito-Lopez, E. Martínez-Gimeno, A. Arnanz, *Organometallics* 2011, *30*, 1838.

33 a) M.J. Abedin, B. Bergman, R. Holmquist, R. Smith, E. Rosenberg, J. Ciurash, K.I. Hardcastle, J. Roe, V. Vazquez, C. Roe, S.E. Kabir, B. Roy, S. Alam, K.A. Azam, *Coord. Chem. Rev.* 1999, *190-192*, 975; b) S.E. Kabir, K.M.A. Malik, H.S. Mandal, Md.A. Mottalib, Md.J. Abedin, E. Rosenberg, *Organometallics* 2002, *21*, 2593; c) Md.A. Mottalib, N. Begum, S.M.T. Abedin, T. Akter, S.E. Kabir, Md.A. Miah, D. Rokhsana, E. Rosenberg, G.M.G. Hossain, K.I. Hardcastle, *Organometallics* 2005, *24*, 4747.

34 K.M. Uddin, S. Ghosh, A.K. Raha, G. Hogarth, E. Rosenberg, A. Sharmin, K.I. Hardcastle, S.E. Kabir, *J. Organomet. Chem.* 2010, *695*, 1435.

35 For a report that contains structurally related clusters based on the addition of DMAD to a pyrone-ligated triomsmium cluster, see: Q. Lin, W.K. Leong, *J. Organomet. Chem.* 2005, *690*, 322.

36 a) S.-H. Huang, J.M. Keith, M.B. Hall, M.G. Richmond, *Organometallics* 2010, *29*, 4041; b) J.C. Sarker, A.K. Raha, S. Ghosh, G. Hogarth, S.E. Kabir, M.G. Richmond, *J. Organomet. Chem.* 2014, *750*, 49.

37 D.M.P. Mingos, D.J. Wales, *Introduction to Cluster Chemistry*, Prentice Hall: Englewood Cliffs, NJ, 1990.

38 F.H. Allen, O. Kennard, D.G. Watson, L. Brammer, A. Orpen, R. Taylor, *J. Chem. Soc., Perkin Trans.* 1987, *2*, S1.

39 M.A.H. Chowdhury, S. Rajbangshi, A. Rahaman, L. Yang, V.N. Nesterov, M.G. Richmond, S.M. Mobin, S.E. Kabir, *J. Organomet. Chem.* 2015, *779*, 21.

40 a) S.E. Kabir, E. Rosenberg, L. Milone, R. Gobetto, D. Osella, M. Ravera, T. McPhillps, M.W. Day, D. Carlot, S. Hajela, E. Wolf, K. Hardcastle, *Organometallics* 1997, *16*, 2674; b) T. Nowroozi-Isfahani, D.G. Musaev, K. Morokuma, E. Rosenberg, *Inorg. Chem.* 2006, *45*, 4963; c) J.A. Cabeza, I. del Río, J.M. Fernández-Colinas, S. García-Granda, L. Martínez-Méndez, E. Pérez-Carreno, *Chem. Eur. J.* 2004, *10*, 6265; d) J.A. Cabeza, I. del Río, S. García-Granda, L. Martínez-Méndez, E. Pérez-Carreno, *Chem. Eur. J.* 2005, *11*, 6040; e) J.A. Cabeza, I. del Río, L. Martínez-Méndez, E. Pérez-Carreno, *Chem. Eur. J.* 2006, *12*, 7694; f) Md.A.H. Chowdhury, Mohd.R. Haque, S. Ghosh, S.M. Mobin, D. A. Tocher, G. Hogarth, M.G. Richmond, S.E. Kabir, H.W. Roesky, *J. Organomet. Chem.* 2017, *836-837*, 68..

41 SMART and SAINT software for CCD diffractometers, version 6.1, Madison, WI, 2000.

42 CrysAlisPRO, Agilent Technologies UK Ltd, Yarnton, England.

43 G.M. Sheldrick, *Acta Cryst.* 2008, *A64*, 112.

44 M.J. Frisch, G.W. Trucks, H.B. Schlegel, G.E. Scuseria, M.A. Robb, J.R. Cheeseman, G. Scalmani, V. Barone, B. Mennucci, G.A. Petersson, H. Nakatsuji, M. Caricato, X. Li, H. P. Hratchian, A.F. Izmaylov, J. Bloino, G. Zheng, J.L. Sonnenberg, M. Hada, M. Ehara, K. Toyota, R. Fukuda, J. Hasegawa, M. Ishida, T. Nakajima, Y. Honda, O. Kitao, H. Nakai, T. Vreven, J. A. Montgomery, Jr., J.E. Peralta, F. Ogliaro, M. Bearpark, J.J. Heyd, E. Brothers, K.N. Kudin, V.N. Staroverov, R. Kobayashi, J. Normand, K. Raghavachari, A. Rendell, J.C. Burant, S.S.


Dalton Transactions Accepted Manuscript



Please do not adjust margins

View Article Online
DOI: 10.1039/C7DT02933K


Iyengar, J. Tomasi, M. Cossi, N. Rega, J.M. Millam, M. Klene, J.E. Knox, J.B. Cross, V. Bakken, C. Adamo, J. Jaramillo, R. Gomperts, R.E. Stratmann, O. Yazyev, A.J. Austin, R. Cammi, C. Pomelli, J.W. Ochterski, R.L. Martin, K. Morokuma, V.G. Zakrzewski, G.A. Voth, P. Salvador, J.J. Dannenberg, S. Dapprich, A. D. Daniels, O. Farkas, J.B. Foresman, J.V. Ortiz, J. Cioslowski, D.J. Fox, Gaussian 09, Revision A.02, Gaussian, Inc., Wallingford CT, 2009.

45 A.D. Becke, *J. Chem. Phys.* 1993, 98, 5648.

46 C. Lee, W. Yang, R.G. Parr, *Phys. Rev. B* 1988, *37*, 785.

47 a) M. Dolg, U. Wedig, H. Stoll, H. Preuss, *J. Chem. Phys.* 1987, 86, 866; b) S.P. Watch, C.W. Bauschlicher, *J. Chem. Phys.* 1983, 78, 4597.

48 a) G.A. Petersson, A. Bennett, T.G. Tensfeldt, M.A. Al-Laham, W.A. Shirley, J. Mantzaris, *J. Chem. Phys.* 1988, 89, 2193; b) G.A. Petersson, M.A. Al-Laham, *J. Chem. Phys.*, 1991, 94, 6081.

49 a) JIMP2, version 0.091, a free program for the visualization and manipulation of molecules: M.B. Hall, R. F. Fenske, *Inorg. Chem.* 1972, 11, 768; b) J. Manson, C.E. Webster, M.B. Hall, Texas A & M University, College Station, TX, 2006: http://www.chem.tamu.edu/jimp2/index.html.

Published on 14 September 2017. Downloaded by University College London on 26/09/2017 10:08:13.

Dalton Transactions Accepted Manuscript


This journal is © The Royal Society of Chemistry 20xx

View Article Online
DOI: 10.1039/C7DT02933K

Published on 14 September 2017. Downloaded by University College London on 26/09/2017 10:08:13.

The reaction of the internal alkyne DEAD with $HOs_3(CO)_9[\mu_3\text{-}C_7H_4NS]$ (**1a**) yields the isomeric alkenyl complexes $Os_3(CO)_9(\mu\text{-}C_7H_4NS)(\mu_3\text{-}EtO_2CCCHCO_2Et)$ (**2a** and **3a**).

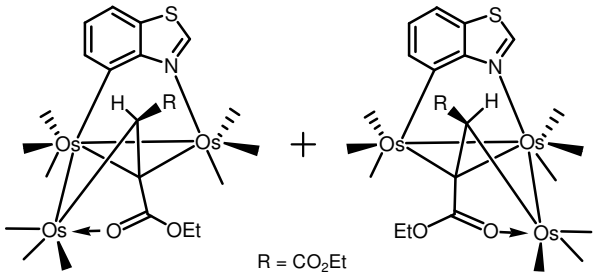


Dalton Transactions Accepted Manuscript